

# Al<sub>3</sub>O<sub>4</sub> and Al<sub>3</sub>O<sub>4</sub><sup>-</sup> Clusters: Structure, Bonding, and Electron Binding Energies

Ana Martínez and Francisco J. Tenorio

*Instituto de Investigaciones en Materiales, UNAM, Circuito Exterior s/n, C. U., P.O. Box 70-360, Coyoacán, 04510, D.F. México*

J. V. Ortiz\*

*Department of Chemistry, Kansas State University, Manhattan, Kansas 66506-3701*

*Received: November 26, 2002; In Final Form: January 30, 2003*

Structure and bonding in neutral and anionic Al<sub>3</sub>O<sub>4</sub> clusters are studied with electronic structure calculations. Geometry optimizations with the B3LYP/6-311+G(2d) density functional method produce several minima, some with distinct multiplicities, for each molecule and anion. The most stable anionic structures are confirmed with additional geometry optimizations at the QCISD level. Equilibrium geometries, harmonic frequencies, and atomic charges are presented. These results, in combination with assignments of photoelectron spectra based on ab initio electron propagator theory, explain the energetic preference of anions for planar structures, while, in contrast, uncharged clusters favor three-dimensional geometries.

## Introduction

Many varieties of chemical bonding between aluminum and oxygen atoms are expressed in the structural, thermodynamic, and reactive properties of ceramics, minerals, nanoparticles, and catalytic supports that contain these two ubiquitous elements. In all of these materials, bonding interactions between oxygen and aluminum are chiefly ionic.<sup>1</sup> In solid phases of Al<sub>2</sub>O<sub>3</sub>, valence electrons of Al are transferred to O atoms, thus producing closed-shell Al<sup>3+</sup> and O<sup>2-</sup> ions whose electrostatic interactions are the principal component of the resulting insulator's cohesive energy. These ionic interactions also are expected in aluminum-rich Al<sub>3</sub>O<sub>y</sub> and Al<sub>3</sub>O<sub>y</sub><sup>-</sup> clusters. Quantum mechanical calculations on molecules and anions where y = 1–3,5 have shown how structure reflects ionic bonding and localization of electrons on aluminum atoms.<sup>2–6</sup>

In a systematic study of anion photoelectron spectra where y = 0–5, Wu et al. reported that the electron affinity of neutral clusters increases with oxygen content.<sup>7,8</sup> Low-energy features in these spectra corresponding to Al-centered orbitals become less numerous and complex as y grows, thus demonstrating the evolution of electronic structure from the metallic case, Al<sub>3</sub><sup>-</sup>, to the oxide limit, Al<sub>3</sub>O<sub>5</sub><sup>-</sup>. Such results suggest that electrons are transferred from aluminum atoms to form closed-shell, oxide dianions. When y = 5, the 10 valence electrons of Al<sub>3</sub><sup>-</sup> are transferred completely to the oxygens and the electron affinity of the corresponding uncharged cluster is especially large. For several of these anions, the presence of more than one isomer has been inferred from the variation of relative peak intensities with respect to laser fluence and ion-source conditions.<sup>7</sup> For the case where y = 3, subsequent computational<sup>9</sup> and experimental<sup>10</sup> studies have considered structures and transition states pertaining to anion photoisomerization. Consideration of the electron detachment energies of more than one anionic isomer therefore is essential for convincing spectral assignments.<sup>2–4</sup>

Photoelectron spectroscopy is an informative probe of molecular electronic structure, but accurate treatments of electron correlation often are needed to produce a quantitative assignment of the most intense spectral features. Determination of the correct order of final states may require correlated levels of theory. Some final states may not correspond even qualitatively to the predictions of uncorrelated methods.

Electron propagator theory provides a framework for the systematic inclusion of correlation in an orbital picture of bonding and spectra.<sup>11</sup> Propagator calculations produce Dyson orbitals and correlated electron binding energies without many-body wave functions or energies of individual states. Several, recently derived propagator approximations have been shown to be accurate and efficient tools for the computation of vertical and adiabatic electron binding energies. The association of Dyson orbitals to these transition energies facilitates interpretation of chemical bonding in terms of familiar concepts.

In previous works,<sup>2,3</sup> we reported ground-state geometries and energies of the low-lying states of neutral and anionic forms of Al<sub>3</sub>O, Al<sub>3</sub>O<sub>2</sub>, Al<sub>3</sub>O<sub>3</sub>, and Al<sub>3</sub>O<sub>5</sub>. Ab initio electron propagator calculations were employed to assign the anion photoelectron spectra of ref 7 and to characterize structure and bonding in these clusters. In a more recent article, optimized geometries, harmonic vibrational frequencies, and atomic charges were examined and trends in isomerization energies of Al<sub>3</sub>O<sub>n</sub> and Al<sub>3</sub>O<sub>n</sub><sup>-</sup> were explained.<sup>4</sup>

In this paper, we discuss stable structures and relative energies of neutral and anionic Al<sub>3</sub>O<sub>4</sub>. Optimized geometries, harmonic vibrational frequencies, atomic charges and isomerization energies are presented. Photoelectron spectra are assigned by comparison with calculated electron detachment energies of anions. Some general structural trends may be discerned in the analysis of these data.

## Computational Methods

All density functional (DF) calculations have been done with the Gaussian 98 program.<sup>12</sup> Geometry optimizations without

\* Corresponding author.

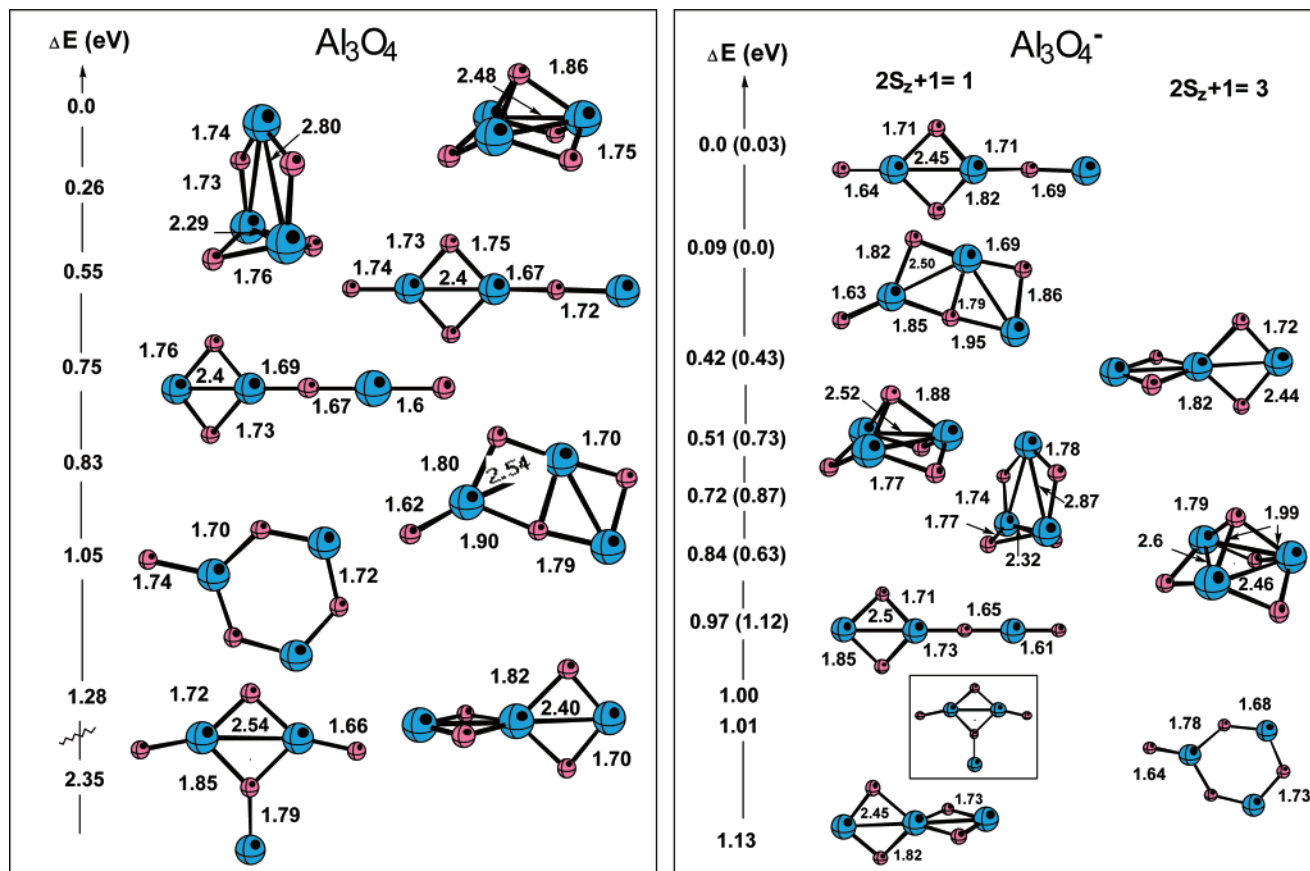


**Figure 1.** Optimized  $\text{Al}_3\text{O}_4$  and  $\text{Al}_3\text{O}_4^-$  structures. Bond distances in Å. B3LYP and QCISD (in parentheses) energy differences in eV.

symmetry constraints were performed with the hybrid B3LYP<sup>13</sup> DF and the 6-311+G(2d) basis.<sup>14</sup> This basis has proven satisfactory in previous studies of aluminum–oxygen clusters.<sup>2,3</sup> Optimized geometries were verified with frequency calculations. To locate distinct minima on potential energy surfaces, optimizations have been started from many initial geometries. Neutral doublets and anionic singlets and triplets were considered. One cannot eliminate the possibility that global or low-lying minima remain undiscovered, but the variety of initial geometries and spin multiplicities investigated here is comparable to that of recent, successful studies of similar clusters.<sup>2–4</sup>

Only the most stable anionic structures from DF calculations were reexamined with *ab initio* geometry optimizations. Quadratic configuration interaction with single and double excitations (QCISD)<sup>15</sup> and 6-311G(d) basis sets were used.<sup>14</sup> (Optimized QCISD geometries obtained with the 6-311G(d) and 6-311+G(2d) basis sets are very similar in test calculations on smaller  $\text{Al}_3\text{O}_n$  clusters.) QCISD geometries were assumed in subsequent electron propagator calculations of the vertical electron detachment energies (VEDEs) of the anions with the 6-311+G(2d) or 6-311+G(2df) basis sets.<sup>14</sup> For the triplet anions, CCSD(T) calculations<sup>15</sup> of VEDEs were performed with the 6-311+G(2df), 6-311+G(2d), or 6-311+G(d) basis sets.

To each VEDE calculated with the electron propagator, there corresponds a Dyson orbital,

$$\Phi_{\text{Dyson}}(x_1) = N^{1/2} \int \Psi_{\text{anion}}(x_1, x_2, x_3, \dots, x_N) \Psi_{\text{neutral}}^*(x_2, x_3, x_4, \dots, x_N) dx_2 dx_3 dx_4 \dots dx_N$$

where  $N$  is the number of electrons in the anion and  $x_i$  is the space–spin coordinate of electron  $i$ . The Dyson orbital thus represents the change in electronic structure associated with

vertical electron detachment. The normalization integral of the Dyson orbital,

$$p = \int |\Phi_{\text{Dyson}}(x)|^2 dx$$

is known as the pole strength. In the zeroth order electron propagator, VEDEs are given by Koopmans's theorem (that is, VEDEs equal negatives of occupied, canonical, Hartree–Fock orbital energies of the anion), Dyson orbitals equal canonical, Hartree–Fock orbitals and pole strengths equal unity. In the present correlated calculations, however, Dyson orbitals are, in general, linear combinations of Hartree–Fock orbitals and pole strengths lie between 0 and 1. Since the Dyson orbitals are subject to a nonlocal, energy-dependent potential known as the self-energy, relaxation and correlation corrections to VEDEs and pole strengths are present in these values. Plots of Dyson orbitals are generated with MOLDEN.<sup>16</sup>

The NR2 and BD-T1 electron propagator approximations are used here.<sup>11</sup> The NR2 method is appropriate for VEDEs of closed-shell species. For ionization energies of typical, organic molecules below 20 eV, average absolute errors are less than 0.2 eV. For species with stronger correlation in the initial state, the BD-T1 method is likely to give superior results. NR2 calculations are performed with the 6-311+G(2df) basis.<sup>14</sup> The more computationally demanding BD-T1 calculations employ the same basis without  $f$  functions.

### Geometry Optimization and Isomerization Energies

Many initial geometries were tested for each structure. For each species, several stationary points were found. Figure 1 presents the most stable neutral and anionic structures. Energetic information from QCISD calculations on anions is shown within parentheses.

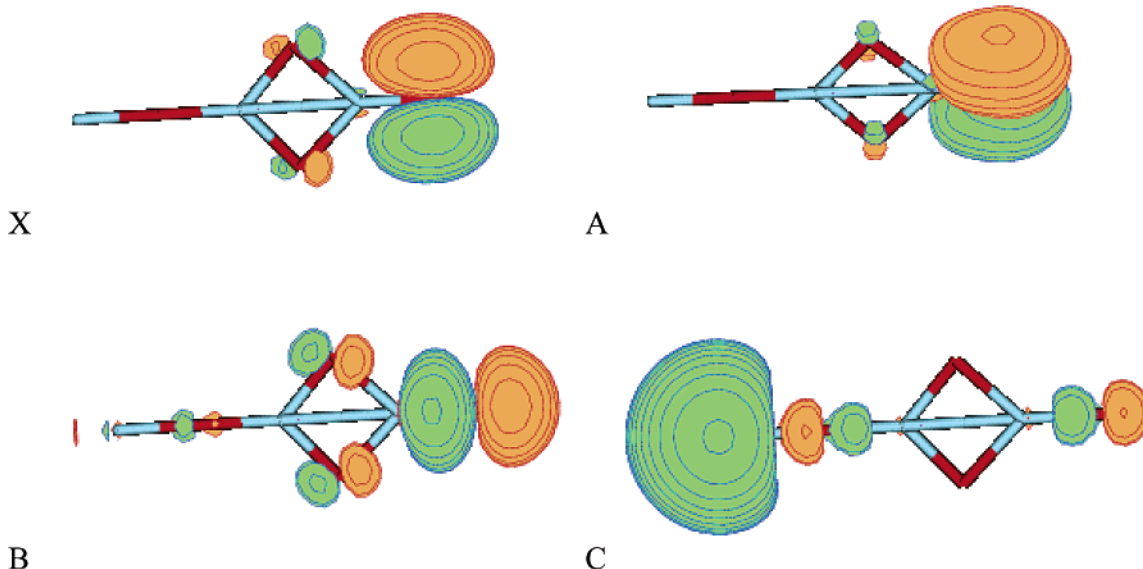


**Figure 2.** Dyson orbitals for VEDEs of  $C_{2v}$  Al<sub>3</sub>O<sub>4</sub><sup>-</sup>. Labels X, A, B, and C refer to final states listed in Table 1.

For Al<sub>3</sub>O<sub>4</sub>, there are two stable, three-dimensional structures, with an energy difference of 0.26 eV. The most stable structure has  $C_{3v}$  symmetry and high coordination numbers for each atom. In the second,  $C_{2v}$  structure, there are two bridging oxygens lying above and below the plane of the three Al nuclei. Somewhat higher in energy are two planar,  $C_{2v}$  isomers with four-member rings consisting of two O and two Al nuclei, followed by another planar structure with  $C_s$  symmetry. More than 1 eV higher than the ground-state lies a structure with a six-member ring and an exocyclic oxygen, a  $D_{2d}$  isomer with four bridging oxygens and a highly unstable structure that resembles a transition state found in the anion.

Al<sub>3</sub>O<sub>4</sub><sup>-</sup> has two structures of comparable stability, with an energy difference of 0.09 eV in DFT calculations. At this level of calculation, the most stable anion is planar and has  $C_{2v}$  symmetry. This structure is similar to the third most stable structure of the neutral. The second most stable isomer bears a strong resemblance to the fifth neutral isomer. At the QCISD level, the order of the two structures changes, but the energy difference is only 0.03 eV. In any case, this value is very small and one cannot say with certainty which isomer is more stable. The lowest triplet has  $D_{2d}$  symmetry and lies approximately 0.4 eV above the  $C_{2v}$  singlet. Nonplanar, anion structures that resemble the two lowest neutral isomers lie 0.5–0.7 eV above the  $C_{2v}$  anion at the DFT level; these figures change to 0.7–0.9 eV with QCISD total energies. There is also another triplet at 0.8 eV (or 0.6 with QCISD). Another singlet that resembles the fourth uncharged minimum was found at 1.12 eV. The figure enclosed in a rectangle at 1.00 eV is a transition state. The nuclear displacement with negative curvature has  $b_2$  symmetry and pertains chiefly to motion of the exocyclic aluminum. Such a transition state lies between the  $C_s$  singlet and its mirror image.

Reoptimized structures at the QCISD/6-311G(d) level are very similar to the DF results. For Al<sub>3</sub>O<sub>4</sub> and Al<sub>3</sub>O<sub>4</sub><sup>-</sup>, several isomers lie within an energy range of 1 eV. Some of these structures play a role in the photoelectron spectra (vide infra).

Three-dimensional geometries are preferred over planar ones for the neutral system, while planar geometries are favored over three-dimensional ones for the anions. In the two lowest isomers of Al<sub>3</sub>O<sub>4</sub>, three-dimensional structures enable all aluminums to have three oxygen neighbors. Each of the oxygens has two aluminum neighbors, with the exception of the apical, tricoordinate oxygen of the  $C_{3v}$  structure. In the planar structures,

**TABLE 1: Vertical Electron Detachment Energies of  $C_{2v}$  Al<sub>3</sub>O<sub>4</sub><sup>-</sup> (eV). Pole Strengths in Parentheses for EPT Calculations**

final state	Koopmans	NR2	BD-T1	expt. [7]
X <sup>2</sup> B <sub>2</sub>	5.06	3.55 (0.87)	3.97 (0.88)	3.9
A <sup>2</sup> B <sub>1</sub>	4.98	3.70 (0.87)	4.12 (0.88)	3.9
B <sup>2</sup> A <sub>1</sub>	6.51	4.78 (0.86)	5.23 (0.91)	5.0
C <sup>2</sup> A <sub>1</sub>	6.35	6.33 (0.91)	6.59 (0.91)	

however, monocoordinate and bicoordinate oxygens and aluminums occur.

**Anion Electron Detachment Energies.** Vertical electron detachment energies (VEDEs) of the two, lowest isomers of Al<sub>3</sub>O<sub>4</sub><sup>-</sup> were evaluated at various levels of electron propagator theory. For the lowest VEDE of the  $C_{2v}$  anion, the best calculation, 3.97 eV, is provided by the BD-T1 approximation and the 6-311+G(2d) basis. Higher VEDEs occur at 4.12 and 5.23 eV. (See Table 1.) All three VEDEs correspond to Dyson orbitals that are dominated by 2p functions on the terminal oxygen atom. (See Figure 2.) Only in the Dyson orbital for the fourth VEDE does one encounter a large contribution from an aluminum-centered orbital. This ordering resembles the results obtained for the kite form of Al<sub>3</sub>O<sub>3</sub><sup>-</sup>, which has the same structure as the  $C_{2v}$  Al<sub>3</sub>O<sub>4</sub><sup>-</sup> singlet except for the absence of a terminal oxygen in the former anion.<sup>2,4</sup> In the Al<sub>3</sub>O<sub>3</sub><sup>-</sup> case, a Dyson orbital centered on the terminal aluminum atom had a higher VEDE than two Dyson orbitals centered on ring oxygens.

In the second singlet, the lowest BD-T1 VEDE occurs at 4.02 eV (see Table 2) and corresponds to a Dyson orbital that is localized chiefly on the Al with only two oxygen neighbors. (See Figure 3.) Antibonding relationships with oxygen 2p functions can be seen in the contours. Dyson orbitals corresponding to subsequent VEDEs at 4.79 and 4.92 eV are centered on the oxygen with only one aluminum neighbor.

Electron correlation affects the ordering of the final states in both isomers. Pole strengths are close to 0.9 and therefore validate the one-electron picture of these VEDEs. NR2 VEDEs are 0.3–0.4 eV smaller.

In the photoelectron spectrum taken with 193 nm radiation,<sup>7</sup> there is a broad peak centered near 3.9 eV with several

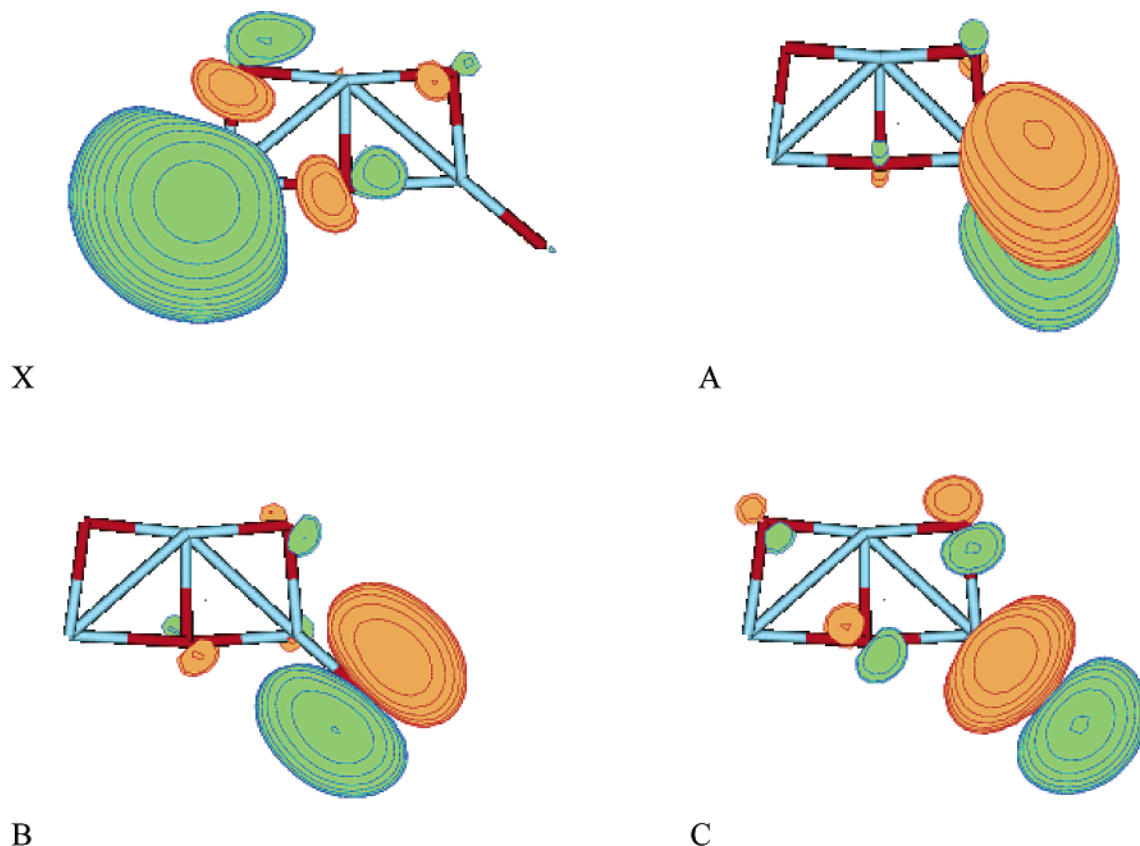


**Figure 3.** Dyson orbitals for VEDEs of  $C_s$   $Al_3O_4^-$ . Labels X, A, B, and C refer to final states listed in Table 2.

**TABLE 2: Vertical Electron Detachment Energies of  $C_s$   $Al_3O_4^-$  (eV). Pole Strengths in Parentheses for EPT Calculations**

final state	Koopmans	NR2	BD-T1	expt [7]
$X^2A'$	3.84	3.69 (0.89)	4.02 (0.90)	3.9
$A^2A''$	5.96	4.42 (0.86)	4.79 (0.88)	5.0
$B^2A'$	5.86	4.55 (0.86)	4.92 (0.88)	5.0
$C^2A'$	7.41	5.67 (0.86)	6.07 (0.87)	

secondary peaks between 3.4 and 4.5 eV. Another prominent peak occurs near 5.0 eV and has subsidiary features from 4.6 to 5.8 eV. The present predictions on the lowest VEDE of the  $C_s$  anion and on the two lowest VEDEs of the  $C_{2v}$  anion suffice to account for the first feature. The second and third VEDEs of the  $C_s$  anion and the third VEDE of the  $C_{2v}$  anion may be assigned to the second broad feature.

VEDEs of other anion isomers were calculated as well. For the  $D_{2d}$   $^3B_2$  anion, VEDEs were evaluated with CCSD(T)/6-311+G(2df) total energies. Values of 3.66, 5.41, and 5.54 were obtained for the  $^2A_1$ ,  $^2B_2$ , and  $^4B_1$  final states, respectively. Estimated error bars of  $\pm 0.2$  eV for the relative energy of the triplet suggest that these VEDEs could be contributing to the two chief features of the 193 nm spectrum. In the triplet, singly occupied  $a_1$  and  $b_2$  spin-orbitals consist chiefly of functions on the terminal aluminums in symmetric or antisymmetric combinations, respectively. QCISD optimizations on a singlet converge to a similar,  $D_{2d}$  structure that has a dominant, closed-shell electron configuration with two electrons assigned to the  $a_1$  orbital. This structure lies 1.1 eV above the lowest singlet and its lowest VEDE obtained with BD-T1 calculations is 4.19 eV.

Photoelectron spectra with longer photon wavelengths have been reported as well.<sup>7</sup> In the 355 nm spectrum, peaks are seen at 1.85, 1.95, and 2.9 eV, while with 266 nm radiation, a feature near 2.05 eV is obtained. In the latter case, a complicated rising pattern of peaks begins near 2.4 eV. The authors state that close examination of the 193 nm spectrum suggests that peaks with extremely weak intensities coincide with the low-energy features seen with longer wavelengths.

None of the VEDEs calculated for the two lowest singlets or the lowest triplet is close to these low-energy peaks. Electron propagator calculations in the BD-T1/6-311+G(2d) approximation obtain VEDEs of 2.38 and 2.32 for the third and fourth singlets. In addition, the VEDE of the second triplet obtained with CCSD(T)/6-311+G(d) total energies is 2.47 eV; this value is likely to increase with the use of larger, more polarized basis sets. These results also employed anion geometries that had been reoptimized with QCISD total energies. The relatively high energies of the three, latter anions (0.6–0.9 eV) imply, however, that they can make only minor contributions to the spectrum. Nayak and Nooijen also considered VEDEs of these species and obtained 4.29, 2.22, and 2.30 eV for structures that resembled the third singlet, the fourth singlet, and the second triplet of the present work.<sup>17</sup>

Given the failure of the high-energy isomers to account for the low-energy features in the 355 and 266 nm spectra, consideration was given to ion–molecule complexes of  $O_2$  and  $Al_3O_2^-$ . The latter anion has two low-lying, planar isomers that both have  $C_{2v}$  symmetry and are within 0.2 eV of each other.<sup>2,4</sup> One structure is a bent Al–O–Al–O–Al chain and the other (called the kite) has a four-member  $Al_2O_2$  ring with an exocyclic Al attached to one of the ring oxygens. QCISD optimizations on  $Al_3O_2^-(O_2)$  complexes (no DFT optimizations were attempted for these anion–molecule complexes) encountered several minima, but the lowest structures for each anionic isomer

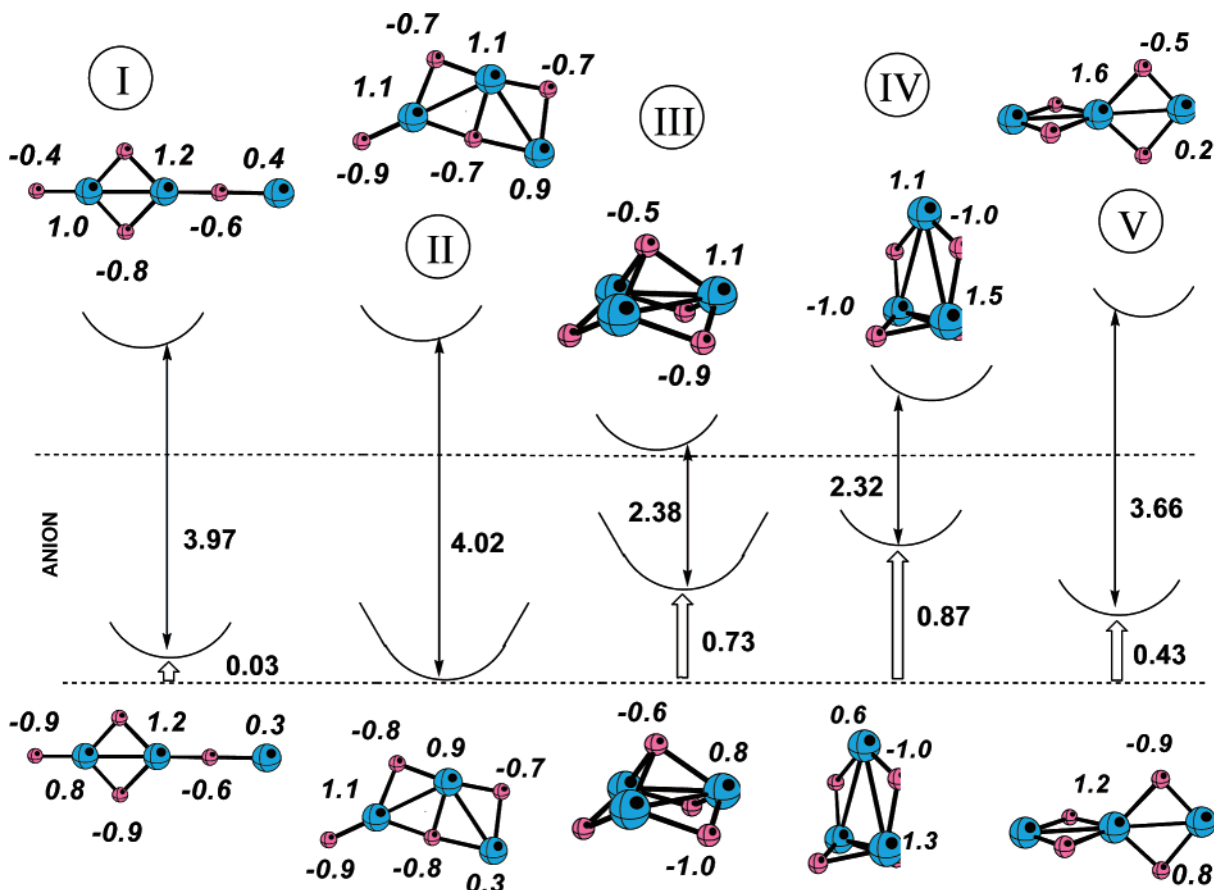


**Figure 4.** Schematic representation of the potential energy surfaces and Mulliken atomic charges for the most stable structures of Al<sub>3</sub>O<sub>4</sub> and Al<sub>3</sub>O<sub>4</sub><sup>-</sup>. Energy differences in eV.

retain  $C_{2v}$  symmetry. Both complexes are planar and the midpoint of the diatomic molecule is bisected by the  $C_2$  axis of the anion in each case. The ground states are triplets, for the multiplicities of the anion and the molecule are singlet and triplet, respectively. For the complex of the chain anion and O<sub>2</sub>, CCSD(T)/6-311+G(2d) calculations produce a VEDE of 1.91 eV for both the lowest doublet and quartet final states. This value may be compared with the 1.8 eV VEDE that was assigned to the chain isomer.<sup>2,4,7</sup> The Dyson orbital for the lowest VEDE is dominated by functions on the central aluminum. The large distance between this aluminum and the midpoint of the O<sub>2</sub> bond, 4.5 Å, implies that the VEDE and its associated Dyson orbital will undergo minimal alteration in the presence of the coordinated molecule. Additional evidence for this interpretation is provided by the nearly identical VEDEs calculated for the doublet and quartet final states. For the complex of the kite isomer of the anion with O<sub>2</sub>, there are VEDEs corresponding to doublet and quartet neutrals at 2.23 eV. In addition, another doublet and another quartet occur at 3.42 eV. For free Al<sub>3</sub>O<sub>2</sub><sup>-</sup>, in comparison, VEDEs at 2.29 and 3.5 eV were assigned to the kite isomer.<sup>2,4,7</sup> Corresponding Dyson orbitals are localized on ring aluminums, not on the exocyclic aluminum that is nearest to the O<sub>2</sub> midpoint in the anion–molecule complex. Here, the distance between the exocyclic aluminum and the midpoint of the coordinated diatomic molecule is also approximately 4.5 Å. The present results on anion–molecule complexes display small shifts in the VEDEs with respect to the uncoordinated anion. Given the ability of the anion source to produce Al<sub>3</sub>O<sub>y</sub><sup>-</sup> clusters with varying  $y$  and the presence of O<sub>2</sub> in the He carrier gas, it seems reasonable to expect that Al<sub>3</sub>O<sub>2</sub><sup>-</sup>(O<sub>2</sub>) clusters containing either

the chain or kite isomers of Al<sub>3</sub>O<sub>2</sub><sup>-</sup> could be responsible for the low-energy peaks from 1.85 to 2.05 eV.

**Trends in Isomerization Energies.** For Al<sub>3</sub>O<sub>4</sub><sup>-</sup>, Figure 4 shows schematic potential energy surfaces for the anionic and neutral clusters. Similar energies were found for the first two singlet anionic structures with DF and QCISD calculations. The calculated VEDE for structure I is 3.97 eV and for structure II this quantity is 4.02 eV. In contrast, VEDEs for the next two singlet anions (III and IV) are 2.38 and 2.32 eV, but their energies relative to the lowest singlet are 0.73 and 0.87 eV, respectively. If one neglects differences in relaxation energies due to nuclear rearrangements in Al<sub>3</sub>O<sub>4</sub>, the neutrals of structures III and IV are expected to be approximately 0.9 eV more stable than those of I and II. Relaxation energies are unlikely to reverse this trend. Thus, planar isomers are favored for Al<sub>3</sub>O<sub>4</sub><sup>-</sup> and the three-dimensional species are favored for Al<sub>3</sub>O<sub>4</sub>. Application of the same kind of arguments to the lowest VEDE (3.66 eV) and the relative energy (0.43 eV) of the  $D_{2d}$  triplet anion indicates that the corresponding neutral cluster lies approximately 0.1 eV above its planar counterparts with structures I and II.

**Vibrational Analysis and Atomic Charges.** Harmonic vibrational frequencies (Tables 3 and 4) and Mulliken atomic charges (Figure 4) have been obtained for the most stable neutral and anionic minima.

In Figure 4, atomic charges in Al<sub>3</sub>O<sub>4</sub> and Al<sub>3</sub>O<sub>4</sub><sup>-</sup> indicate that the oxygen atoms are negative, as one would expect from the electronegativities of oxygen and aluminum. If one compares the neutral and the anion of structure III, the charges of the aluminums that are equivalent by symmetry in the anion are 0.8, whereas in the neutral system these charges are 1.1. Charges

**TABLE 3: Calculated Harmonic Vibrational Frequencies (in  $\text{cm}^{-1}$ ) of Low-Energy Isomers of  $\text{Al}_3\text{O}_4$** 

$\text{Al}_3\text{O}_4$	Harmonic Frequencies ( $\text{cm}^{-1}$ )							
	228	229	313	314	326	505	506	560
	e	e	e	e	$a_1$	e	e	e
	561	569	654	697	717	799	800	
	e	$a_1$	$a_1$	$a_2$	$a_1$	e	e	
	102	252	268	275	331	442	569	573
	$b_1$	$a_1$	$b_2$	$a_2$	$b_1$	$a_1$	$a_1$	$a_1$
	631	641	740	756	756	792	845	
	$b_2$	$a_1$	$a_1$	$b_1$	$b_2$	$b_2$	$a_1$	
	35	44	113	164	232	247	318	396
	$b_2$	$b_1$	$b_1$	$b_2$	$b_1$	$b_2$	$a_1$	$b_1$
	537	666	708	792	807	925	1074	
	$a_1$	$b_2$	$a_1$	$a_1$	$b_2$	$a_1$	$a_1$	
	32	44	147	176	238	259	313	362
	$b_2$	$b_1$	$b_1$	$b_2$	$b_1$	$b_2$	$a_1$	$b_1$
	587	643	740	779	809	1026	1213	
	$a_1$	$b_2$	$a_1$	$b_2$	$a_1$	$a_1$	$a_1$	
	83	142	170	258	271	332	379	445
	$a'$	$a'$	$a'$	$a'$	$a'$	$a'$	$a'$	$a'$
	588	596	614	687	740	962	1039	
	$a'$	$a'$	$a'$	$a'$	$a'$	$a'$	$a'$	

on the oxygen atoms are  $-1.0$  and  $-0.6$  for the anionic system and become  $-0.9$  and  $-0.5$  for the neutral. Aluminum atoms are more positive in the neutral system. Therefore, the Coulombic attraction energy between aluminum and oxygen atoms is more pronounced for the neutral than for the anionic structure. For the neutral system, structure III is the most stable isomer because Coulombic attractions are accentuated by enhanced atomic charges and high coordination numbers. The same behavior is obtained for structure IV. If one compares the neutral and anion of structure IV, the charges of the aluminums are 1.3 and 0.6, whereas in the neutral system these charges are 1.5 and 1.1. The charges on the oxygen atoms are  $-1.0$  for both systems. Because of the more positive charge on the aluminum atoms in the neutral system, the Coulombic attraction energy between aluminum and oxygen atoms is more pronounced for the neutral than for the anionic structure. For the neutral system, enhanced Coulombic interactions favor structures III and IV with respect to the planar isomers.

Dyson orbitals corresponding to the lowest VEDEs of each isomer are compatible with the corresponding changes in atomic charges. For example, for the lowest VEDE of the lowest  $C_{2v}$  anion, the Dyson orbital is concentrated on the monocoordinate oxygen, which is also the site that loses 0.5 electrons in the Mulliken scheme. For the  $C_s$  anion, the Dyson orbital for the lowest VEDE is localized on the bicoordinate aluminum, which loses 0.6 electrons. In the remaining structures of Figure 4, the Dyson orbitals for the lowest VEDEs consist chiefly of functions on the sites with the lowest coordination numbers and the largest changes in Mulliken charges also occur in these positions.

**TABLE 4: Calculated Harmonic Vibrational Frequencies (in  $\text{cm}^{-1}$ ) of Low-Energy Isomers of  $\text{Al}_3\text{O}_4^-$** 

$\text{Al}_3\text{O}_4^-$	Harmonic Frequencies ( $\text{cm}^{-1}$ )							
	21	38	116	202	258	273	311	394
	$b_2$	$b_1$	$b_1$	$b_2$	$b_1$	$b_2$	$a_1$	$b_1$
	541	554	648	840	858	1025	1070	
	$a_1$	$b_2$	$a_1$	$b_2$	$a_1$	$a_1$	$a_1$	
	95	137	164	253	269	379	387	399
	$a'$	$a'$	$a'$	$a'$	$a'$	$a'$	$a'$	$a'$
	496	567	652	688	747	1005	1055	
	$a'$	$a'$	$a'$	$a'$	$a'$	$a'$	$a'$	
	122	122	156	317	335	335	539	539
	$b_1$	$b_2$	$a_2$	$a_1$	$b_1$	$b_2$	$b_1$	$b_2$
	553	629	743	793	793	810	813	
	$a_1$	$a_1$	$a_1$	$b_2$	$b_1$	$a_1$	$a_1$	
	226	226	314	315	315	478	478	544
	e	e	$a_1$	e	e	e	e	e
	544	554	616	654	694	762	762	
	e	$a_1$	$a_1$	$a_2$	$a_1$	e	e	
	112	220	236	263	320	430	534	537
	$b_1$	$b_2$	$a_1$	$a_2$	$b_1$	$a_1$	$a_1$	$a_2$
	545	558	679	697	722	743	801	
	$b_2$	$a_1$	$b_2$	$a_1$	$b_1$	$b_2$	$a_1$	

## Conclusions

Density functional optimizations produce a three-dimensional,  $C_{3v}$  structure for doublet  $\text{Al}_3\text{O}_4$  and two, planar, approximately isoenergetic singlets for  $\text{Al}_3\text{O}_4^-$ . A low-lying triplet with  $D_{2d}$  symmetry was found as well. Distinct patterns of stability occur for the neutral and anionic structures. For  $\text{Al}_3\text{O}_4^-$ , planar structures I and II are more stable than the three-dimensional isomers. For neutral  $\text{Al}_3\text{O}_4$ , three-dimensional structures III and IV are clearly lower in energy than the planar ones.

Electron propagator results for the VEDEs of the two lowest structures of  $\text{Al}_3\text{O}_4^-$  are in close agreement with photoelectron spectra. Dyson orbitals pertaining to these ionizations may be concentrated on aluminum or oxygen atoms with low coordination number. In one isomer, the lowest VEDE pertains to an aluminum-centered Dyson orbital, whereas in the other case, the Dyson orbital for the lowest VEDE is concentrated on an exocyclic oxygen. The lowest triplet anion and two relatively unstable singlets may also contribute to the photoelectron spectrum. VEDEs of  $\text{Al}_3\text{O}_2^-(\text{O}_2)$  complexes are close to the observed, low-energy features seen in spectra produced with longer-wavelength radiation.

Vibrational frequencies and Mulliken atomic charges were reported for the more stable neutral and anionic minima. The stability order of the anionic and neutral compounds may be explained by Coulombic attractions and repulsions between

aluminum and oxygen atoms. In the anions, aluminum atoms have smaller positive charges than in the neutrals and electrostatic attractions with negatively charged oxygens are weaker. In the neutrals, three-dimensional structures are favored, for the ions have higher coordination numbers. Planar structures have more atoms with low coordination numbers and are favored by the anions. Thus, the uncharged clusters bear a closer resemblance to the three-dimensional structure of ionic bonds found in bulk phases. In the anions, separation of negative charges leads to a preference for planar geometries.

**Acknowledgment.** The authors acknowledge Sara Jiménez Cortés and María Teresa Vázquez for technical support and DGSCA/UNAM (México) for providing computer time. This work was partially funded by DGAPA (# IN107399) and CONACYT-NSF (E120.1778/2001). J.V.O. acknowledges support from the National Science Foundation (Grants CHE-9873897 and CHE-0135823) and Kansas DEPSCoR. We thank Prof. Marcel Nooijen of Princeton University for sending us the results of ref 17.

## References and Notes

- (1) Henrich, V. E.; Cox, P. A. *The Surface Science of Metal Oxides*; Cambridge University Press: New York, 1994.
- (2) Martínez, A.; Tenorio, F. J.; Ortiz, J. V. *J. Phys. Chem. A* **2001**, *105*, 8787.
- (3) Martínez, A.; Tenorio, F. J.; Ortiz, J. V. *J. Phys. Chem. A* **2001**, *105*, 11291.
- (4) Martínez, A.; Sansores, L. E.; Salcedo, R.; Tenorio, F. J.; Ortiz, J. V. *J. Phys. Chem. A* **2002**, *106*, 10630.
- (5) Ghanty, T. K.; Davidson, E. R. *J. Phys. Chem. A* **1999**, *103*, 2867.
- (6) Ghanty, T. K.; Davidson, E. R. *J. Phys. Chem. A* **1999**, *103*, 8985.
- (7) Wu, H.; Li, X.; Wang, X.-B.; Ding, C.-F.; Wang, L.-S. *J. Chem. Phys.* **1998**, *109*, 449.
- (8) Desai, S. R.; Wu, H.; Wang, L.-S. *Int. J. Mass Spectrom. Ion Processes* **1996**, *159*, 75.
- (9) Cui, X. Y.; Morrison, I.; Han, J.-G. *J. Chem. Phys.* **2002**, *117*, 1077.
- (10) Akin, F. A.; Jarrold, C. C. *J. Chem. Phys.* **2003**, *118*, 1773.
- (11) (a) Ortiz, J. V. In *Computational Chemistry: Reviews of Current Trends*; Leszczynski, J., Ed.; World Scientific: Singapore, 1997; Vol. 2, p 1. (b) Ortiz, J. V. *Adv. Quantum Chem.* **1999**, *35*, 33. (c) Ortiz, J. V.; Zakrzewski, V. G.; Dolgoumitcheva, O. In *Conceptual Trends in Quantum Chemistry*; Kryachko, E. S., Ed.; Kluwer: Dordrecht, 1997; Vol. 3, p 465.
- (12) Frisch, M. J.; Trucks, G. W.; Schlegel, H. B.; Scuseria, G. E.; Robb, M. A.; Cheeseman, J. R.; Zakrzewski, V. G.; Montgomery, J. A., Jr.; Stratmann, R. E.; Burant, J. C.; Dapprich, S.; Millam, J. M.; Daniels, A. D.; Kudin, K. N.; Starin, M. C.; Farkas, O.; Tomasi, J.; Barone, V.; Cossi, M.; Cammi, R.; Mennucci, B.; Pomelli, C.; Adamo, C.; Clifford, S.; Ochterski, J.; Petersson, G. A.; Ayala, P. Y.; Cui, Q.; Morokuma, K.; Malick, D. K.; Rabuck, A. D.; Raghavachari, K.; Foresman, J. B.; Cioslowski, J.; Ortiz, J. V.; Stefanov, B. B.; Liu, G.; Liashenko, A.; Piskorz, P.; Komaromi, I.; Gomperts, R.; Martin, R. L.; Fox, D. J.; Keith, T.; Al-Laham, M. A.; Peng, C. Y.; Nanayakkara, A.; González, C.; Challacombe, M.; Gill, P. M. W.; Chen, W.; Wong, M. W.; Andres, J. L.; Head-Gordon, M.; Replogle, E. S.; Pople, J. A. *GAUSSIAN 98*, Revisión A8; Gaussian Inc.: Pittsburgh, PA, 1998.
- (13) (a) Becke, A. D. *J. Chem. Phys.* **1993**, *98*, 5648. (b) Lee, C.; Yang, W.; Parr, R. G. *Phys. Rev. B* **1988**, *37*, 785. (c) Mielich, B.; Savin, A.; Stoll, H.; Preuss, H. *Chem. Phys. Lett.* **1989**, *157*, 200.
- (14) (a) Krishnan, R.; Binkley, J. S.; Seeger, R.; Pople, J. A. *J. Chem. Phys.* **1980**, *72*, 650. (b) Clark, T.; Chandrasekhar, J.; Spitznagel, G. W.; Schleyer, P. v. R. *J. Comput. Chem.* **1983**, *4*, 294. (c) Frisch, M. J.; Pople, J. A.; Binkley, J. S. *J. Chem. Phys.* **1984**, *80*, 3265. (d) McLean, A. D.; Chandler, G. S. *J. Chem. Phys.* **1980**, *72*, 5639.
- (15) Pople, J. A.; Head-Gordon, M.; Raghavachari, K. *J. Chem. Phys.* **1987**, *87*, 5968.
- (16) Schaftenaar, G. *MOLDEN 3.4*, CAOS/CAMM Center, The Netherlands.
- (17) Nayak, S. K.; Nooijen, M. Private communication.